



## Communication

## A ratiometric merocyanine-based fluorescent probe for detecting hydrazine in living cells and zebra fish



Jinliang Han<sup>a</sup>, Xiuxiu Yue<sup>a</sup>, Jingpei Wang<sup>a</sup>, Yun Zhang<sup>a</sup>, Benhua Wang<sup>a,\*</sup>,  
Xiangzhi Song<sup>a,b,\*</sup>

<sup>a</sup> College of Chemistry & Chemical Engineering, Central South University, Changsha 410083, China

<sup>b</sup> Key Laboratory of Hunan Province for Water Environment and Agriculture Product Safety, Changsha 410083, China

## ARTICLE INFO

## Article history:

Received 5 November 2019

Received in revised form 9 January 2020

Accepted 10 January 2020

Available online 14 January 2020

## Keywords:

Fluorescent probe

Hydrazine

Merocyanine

Ratiometric

Cell imaging

## ABSTRACT

We developed a merocyanine-based fluorescent probe, NEPB, for tracing hydrazine ( $N_2H_4$ ) in a ratiometric manner with large Stokes shifts and long emission wavelength. The fluorescence color of probe NEPB changed from green to yellow upon addition of hydrazine. Probe NEPB displayed high selectivity and sensitivity to hydrazine in solution, and could ratiometrically monitor  $N_2H_4$  in living cells and zebrafish with low cytotoxicity.

© 2020 Chinese Chemical Society and Institute of Materia Medica, Chinese Academy of Medical Sciences.

Published by Elsevier B.V. All rights reserved.

Hydrazine ( $N_2H_4$ ) is a significant industrial material and play important roles in chemical, pharmaceutical and agricultural areas [1,2], such as catalysts, corrosion inhibitor and pharmaceutical intermediates because of its basic and reductive properties [3,4]. In addition, it is widely used as high energy fuel in aerospace and military industry for its explosive characteristics [5–11]. Despite being very useful, it is a highly toxic and carcinogenic compound, which could cause serious damages to human lungs, liver, kidneys, and the central nervous system [12–15]. Therefore, it is necessary to provide reliable analytical methods to monitor  $N_2H_4$  with high sensitivity and selectivity.

Various different analytical methods for determining hydrazine have been reported, including chromatography [16,17], titrimetry [7], electrochemistry [18,19], and so forth. However, these methods are limited by many factors, such as time consuming, complicated sample handling processes and poor compatibility in biological systems, which extremely restrict the application in living cells [15,20]. Recently, fluorescent probes had been paid close attention due to their satisfactory selectivity, low cost, and non-invasive detection in organism systems [8,21]. Over the past several years, a number of probes for hydrazine have been reported [2,9,22–24],

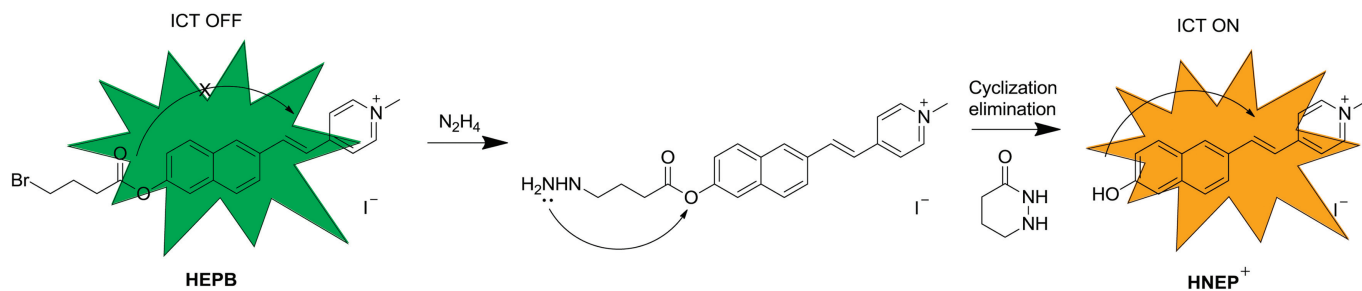
but most of them are turn-on types with small Stokes shifts. It is known to us that the fluorescence intensity-based probes can be easily influenced by auto-fluorescence and unpredictable instrumental factors [25–27]. To circumvent this problem, ratiometric fluorescent probes that functioned through two signal outputs were developed to eliminate the interfering factors [15,28–32]. To avoid two emission bands overlapping and make the probe more suitable in bioassays, large Stokes shifts (>60 nm) and long emission wavelength are desired.

In view of these above factors, we used merocyanine derivative (HNEP<sup>+</sup>) as the fluorophore and 4-bromobutyric acid as the reaction site [15] and constructed a novel probe NEPB for hydrazine. As shown in Scheme 1, intramolecular charge transfer (ICT) process played important part in the construction of ratiometric probes. Here, 4-bromobutyric acid also acted as an electron-withdrawing group and blocked the ICT process of the fluorophore. When probe NEPB reacted with  $N_2H_4$ , a substitution-cyclisation-elimination reaction happened at the recognizing site and released fluorophore HNEP<sup>+</sup>, which exhibited the ICT properties with large Stokes shifts and long emission wavelength. Probe NEPB was easily prepared within three steps as shown in Scheme S1 (Supporting information) and characterized by standard <sup>1</sup>H NMR, <sup>13</sup>C NMR and HRMS spectra (Supporting information).

At the first step, we investigated the absorption and fluorescence properties of probe NEPB in DMSO/PBS buffer (9:1, v/v, 10.0 mmol/L, pH 7.4). As shown in Fig. S1 (Supporting information),

\* Corresponding authors at: College of Chemistry & Chemical Engineering, Central South University, Changsha 410083, China.

E-mail addresses: [benhuawang@csu.edu.cn](mailto:benhuawang@csu.edu.cn) (B. Wang), [song@rowland.harvard.edu](mailto:song@rowland.harvard.edu) (X. Song).



**Scheme 1.** The recognition mechanism of probe NEPB towards  $N_2H_4$ .

the free probe NEPB displayed an absorption band at 360 nm. Upon reaction with excessive  $N_2H_4$ , the absorption band red-shifted to 413 nm, with the solution changed from pale-green to yellow, which was attributed to the ICT process. Probe NEPB exhibited strong green fluorescence with a maximum emission at 501 nm. When treated with  $N_2H_4$ , an intramolecular cyclization reaction happened at the ester site, which would release the yellow fluorophore of HNEP<sup>+</sup> with an emission at 575 nm. These results demonstrated that probe NEPB could serve as a ratiometric fluorescent sensor to detect  $N_2H_4$ .

To evaluate the sensitivity of probe NEPB to  $N_2H_4$ , different amounts of  $N_2H_4$  (0.0–1000.0  $\mu\text{mol/L}$ ) were added into the solution of NEPB. It was seen in Fig. 1A that the fluorescence intensity of probe NEPB at 501 nm reduced, and the intensity at 575 nm increased with the addition of incremental doses of  $N_2H_4$ , and it was finally saturated with 200.0 equiv. of  $N_2H_4$ . In addition, the fluorescence intensity was linearly related to the concentration of  $N_2H_4$  in the range of 0–700.0  $\mu\text{mol/L}$  (Fig. 1B). The detection limit for  $N_2H_4$  was estimated to be 2.6  $\mu\text{mol/L}$  ( $S/N=3$ ), which indicates that NEPB could quantitatively detect  $N_2H_4$  with good sensitivity.

Then the time-dependent fluorescence properties of probe NEPB in the absence/presence of  $N_2H_4$  were carried out. As shown in Fig. S3 (Supporting information), a gradual increase at 575 nm and a simultaneous decline at 501 nm were observed as the time went on. The reaction could be detected within 10 min and reached a plateau around 120 min when probe NEPB was reacted with 1000.0  $\mu\text{mol/L}$  of  $N_2H_4$ .

In order to determine whether probe NEPB can operate well under physiological condition, the fluorescence behavior was investigated under different pH values in the absence/presence of  $N_2H_4$ . As shown in Fig. S4 (Supporting information), the fluorescence intensity ratio ( $I_{575}/I_{501}$ ) of probe NEPB was almost no change in a wide pH range of 2–10, demonstrating that free probe NEPB was quite stable. However, the ratio dramatically increased within pH 6–11 in the presence of  $N_2H_4$ , suggesting that it is suitable for probe NEPB to detect  $N_2H_4$  in physiological condition.

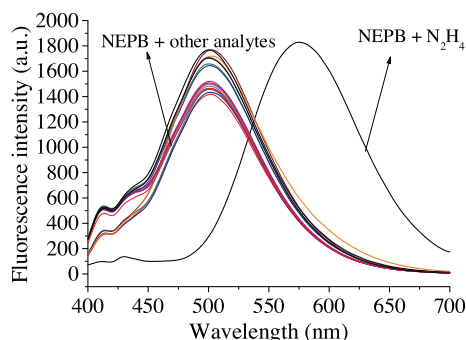


**Fig. 2.** Fluorescence spectra of probe NEPB (5.0  $\mu\text{mol/L}$ ) in the presence of various biological species (1.0 mmol/L): (1)  $Na^+$ ; (2)  $Zn^{2+}$ ; (3)  $Al^{3+}$ ; (4)  $Co^{2+}$ ; (5)  $Ca^{2+}$ ; (6)  $Ba^{2+}$ ; (7)  $K^+$ ; (8)  $NO^-$ ; (9)  $HSO_3^-$ ; (10)  $SO_3^{2-}$ ; (11)  $Br^-$ ; (12)  $HCO_3^-$ ; (13)  $SO_4^{2-}$ ; (14)  $S_2O_5^{2-}$ ; (15)  $S_2O_3^{2-}$ ; (16)  $NH_3$ ; (17)  $N_2H_4$ .

Next, we checked the specificity of probe NEPB for  $N_2H_4$  over other competitive analytes. The fluorescence changes of probe NEPB were evaluated in the presence of various relevant species, including  $Na^+$ ,  $Zn^{2+}$ ,  $Al^{3+}$ ,  $Co^{2+}$ ,  $Ca^{2+}$ ,  $Ba^{2+}$ ,  $K^+$ ,  $NO^-$ ,  $HSO_3^-$ ,  $SO_3^{2-}$ ,  $Br^-$ ,  $HCO_3^-$ ,  $SO_4^{2-}$ ,  $S_2O_5^{2-}$ ,  $S_2O_3^{2-}$ ,  $NH_3$  and  $N_2H_4$ . As depicted in Fig. 2, only  $N_2H_4$  could result a significant increase in the fluorescence intensity at 575 nm and dramatic decrease at 501 nm, whereas other species did cause little spectral changes. What is more, the competitive experiments also demonstrated that the above interfering species did not affect the fluorescence performance of probe NEPB toward  $N_2H_4$  (Fig. S2 in Supporting information). These results confirmed that probe NEPB could be used to detect  $N_2H_4$  selectively.

Afterwards, to confirm the sensing mechanism, the reaction products of probe NEPB with  $N_2H_4$  was analyzed by high resolution mass spectrometry (Fig. S6 in Supporting information). It was found that two new peaks appeared at  $m/z$  123.0930 and 262.1244, which were exactly identical to the dye HNEP<sup>+</sup> ( $[M]^+ = 262.1226$ ) and by-product tetrahydro-pyridazin-3-one ( $[M + Na]^+ = 123.0915$ ). This

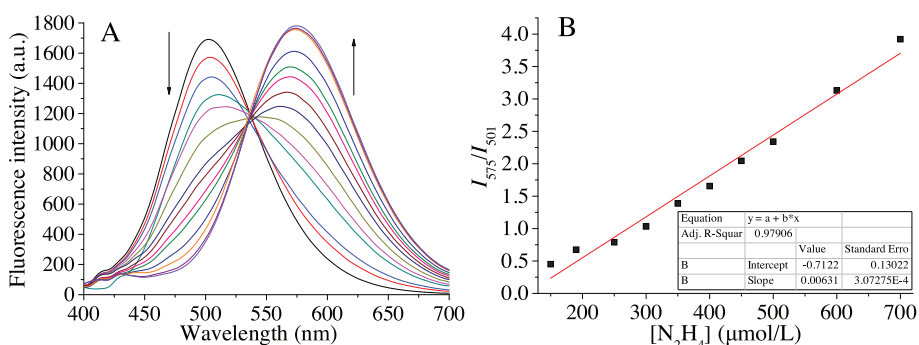


**Fig. 1.** (A) Normalized absorption and (B) fluorescence emission spectra of probe NEPB (5.0  $\mu\text{mol/L}$ ) in the absence (black) and presence (red) of  $N_2H_4$  (200.0 equiv.) in DMSO/PBS buffer (9:1, v/v, 10 mmol/L, pH 7.4).  $\lambda_{\text{ex}} = 380$  nm.

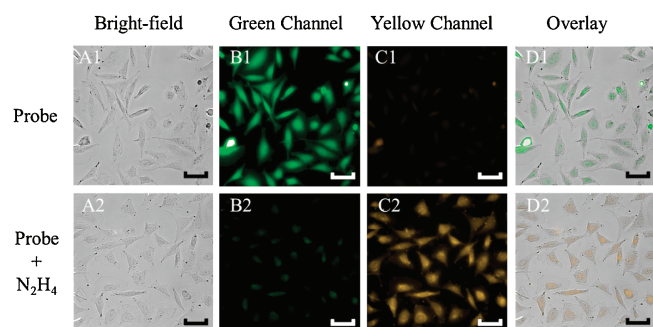


**Fig. 3.** Fluorescence and bright field images of cells. (A1–D1): Cells incubated with probe NEPB (5.0  $\mu\text{mol/L}$ ) for 30 min. (A2–D2): Cells treated with probe NEPB (5.0  $\mu\text{mol/L}$ ) and then incubated with  $\text{N}_2\text{H}_4$  (1000.0  $\mu\text{mol/L}$ ) for 2 h. Green channel was collected from 500 nm to 550 nm and yellow channel was collected from 570 nm to 620 nm.  $\lambda_{\text{ex}} = 390\text{--}420\text{ nm}$ . Scale bar = 20  $\mu\text{m}$ .

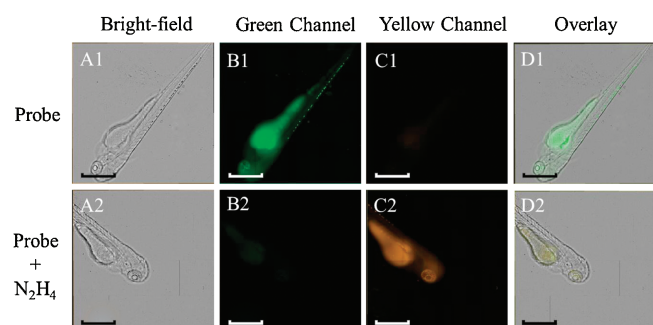


**Fig. 4.** Images of NEPB in 3-day-old zebra fish. (A1–D1): Zebra fish incubated with probe NEPB (5.0  $\mu\text{mol/L}$ ) for 30 min. (A2–D2): Zebra fish treated with probe NEPB (5.0  $\mu\text{mol/L}$ ) and then incubated with  $\text{N}_2\text{H}_4$  (1000.0  $\mu\text{mol/L}$ ) for 2 h. Green channel was collected from 500 nm to 550 nm and yellow channel was collected from 570 nm to 620 nm.  $\lambda_{\text{ex}} = 390\text{--}420\text{ nm}$ . Scale bar = 500  $\mu\text{m}$ .

result was in good agreement with the proposed sensing process in Scheme 1.

Encouraged by the above results, the capacity of probe NEPB to detect  $\text{N}_2\text{H}_4$  in living cells was then assessed. We first used the conventional MTT assay with HeLa cells to evaluate the cytotoxicity of probe NEPB. As shown in Fig. S5 (Supporting information), the cell viability exceeded 86% when the cells were treated with 20.0  $\mu\text{mol/L}$  of probe NEPB for 24 h, indicating that probe NEPB was almost non-toxicity and suitable for biological applications.

In the following steps, practical applications of probe NEPB in living HeLa cells and zebra fish were investigated. As shown in Fig. 3, we observed a strong fluorescence in green channel and an ignorable fluorescence in yellow channel when cells only treated with probe NEPB (5.0  $\mu\text{mol/L}$ ). With the addition of  $\text{N}_2\text{H}_4$ , a strong fluorescence appeared in yellow channel, and accompanied by the reduction of fluorescence in green channel. These results indicated that probe NEPB had the ability to monitor  $\text{N}_2\text{H}_4$  in living cells. Inspired by the good performance in living cells, the imaging experiments in zebra fish were further carried out. To our delight, the phenomena in NEPB-treated zebra fish were consistent with the above cell imaging experiments (Fig. 4). These findings clearly demonstrated the ability of probe NEPB to detect  $\text{N}_2\text{H}_4$  via dual distinct emission bands in living systems.

In conclusion, we have designed and synthesized a novel ratiometric fluorescent probe NEPB with large Stokes shift and long emission wavelength for the detection of  $\text{N}_2\text{H}_4$ . Probe NEPB displayed high sensitivity and selectivity as well as low detection limit towards  $\text{N}_2\text{H}_4$ . Additionally, probe NEPB was successfully applied for detecting  $\text{N}_2\text{H}_4$  in living cells and zebra fish. Considering these, we believed that the probe would have a good potential to act as a valuable tool to detect  $\text{N}_2\text{H}_4$  in environmental pollution and living systems.

#### Declaration of competing interest

The authors declare that they have no known competing financial interests or personal relationships that could have appeared to influence the work reported in this paper

#### Acknowledgments

This work was supported by the National Natural Science Foundation of China (No. U1608222), Special Fund for Agro-scientific Research in the Public Interest of China (No. 201503108), the Fundamental Research Funds for the Central Universities of Central South University (Nos. 2019zzts438, 2019zzts846) and the State Key Laboratory of Chemo/Biosensing and Chemometrics (No. 2016005).

#### Appendix A. Supplementary data

Supplementary material related to this article can be found, in the online version, at doi:<https://doi.org/10.1016/j.ccllet.2020.01.029>.

#### References

- [1] W.Z. Xu, W.Y. Liu, T.T. Zhou, et al., *Spectrochim. Acta A* 193 (2018) 324–329.
- [2] G. Li, Y. Liu, J. Song, et al., *J. Fluoresc.* 27 (2017) 323–329.
- [3] J.Y. Wang, Z.R. Liu, M. Ren, W. Lin, *Sci. Rep.* 7 (2017) 1530–1537.
- [4] K.F. Khaled, *Appl. Surf. Sci.* 252 (2006) 4120–4128.
- [5] Y. Qian, J. Lin, L. Han, et al., *Biosens. Bioelectron.* 58 (2014) 282–286.
- [6] C. Hu, W. Sun, J. Cao, et al., *Org. Lett.* 15 (2013) 4022–4025.
- [7] Z. Li, W. Zhang, C. Liu, et al., *Sens. Actuators B* 241 (2017) 665–671.
- [8] Z. Lu, W. Fan, X. Shi, et al., *Anal. Chem.* 89 (2017) 9918–9925.
- [9] B. Shi, Y. He, P. Zhang, et al., *Dyes Pigm.* 147 (2017) 152–159.
- [10] J.W. Mo, B. Ogorevc, X. Zhang, et al., *Electroanalysis* 12 (2000) 48–54.
- [11] Q. Wu, J. Zheng, W. Zhang, et al., *Talanta* 195 (2019) 857–864.
- [12] J. Zhang, L. Ning, J. Liu, et al., *Anal. Chem.* 87 (2015) 9101–9107.
- [13] C.A. Reilly, S.D. Aust, *Chem. Res. Toxicol.* 10 (1997) 328–334.
- [14] J. Liu, J. Shen, M. Li, L.P. Guo, *Chin. Chem. Lett.* 26 (2015) 1478–1484.
- [15] Y. Hao, Y. Zhang, K. Ruan, et al., *Sens. Actuators B* 244 (2017) 417–424.
- [16] D.P. Elder, D. Snodin, A. Teasdale, *J. Pharm. Biomed. Anal.* 54 (2011) 900–910.
- [17] Y.Y. Liu, I. Schmeltz, D. Hoffmann, *Anal. Chem.* 46 (1974) 885–889.
- [18] S. Daemi, A.A. Ashkarran, A. Bahari, et al., *Sens. Actuators B* 245 (2017) 55–65.
- [19] L. Wang, Q. Teng, X. Sun, et al., *J. Colloid Interface Sci.* 512 (2018) 127–133.
- [20] Y. Gao, Y. Lin, T. Liu, et al., *Chin. Chem. Lett.* 30 (2019) 63–66.
- [21] Y. Yang, Q. Zhao, W. Feng, et al., *Chem. Rev.* 113 (2013) 192–270.
- [22] S. Wang, S. Ma, J. Zhang, et al., *Sens. Actuators B* 261 (2018) 418–424.
- [23] T. Tang, Y.Q. Chen, B.S. Fu, et al., *Chin. Chem. Lett.* 27 (2016) 540–544.
- [24] Q. Fang, L. Yang, H. Xiong, et al., *Chin. Chem. Lett.* 31 (2020) 129–132.
- [25] H.H. Xiong, L. He, Y. Zhang, et al., *Chin. Chem. Lett.* 30 (2019) 1075–1077.
- [26] J. Fan, W. Sun, M. Hu, et al., *Chem. Commun.* 48 (2012) 8117–8119.
- [27] Y. Hao, Y. Zhang, K. Ruan, et al., *Spectrochim. Acta A* 184 (2017) 355–360.
- [28] S.I. Reja, N. Gupta, V. Bhalla, et al., *Sens. Actuators B* 222 (2016) 923–929.
- [29] Z. Xu, M. Pang, C. Li, et al., *Luminescence* 32 (2017) 466–470.
- [30] J. Wu, J. Pan, Z. Ye, et al., *Sens. Actuators B* 274 (2018) 274–284.
- [31] C. Zhao, X. Zhang, K. Li, et al., *J. Am. Chem. Soc.* 137 (2015) 8490–8498.
- [32] S. Goswami, S. Das, K. Aich, et al., *Org. Lett.* 15 (2013) 5412–5415.